RSC Advances

PAPER

View Article Online
View Journal | View Issue

Cite this: *RSC Adv.*, 2022, **12**, 33304

A series of *N*-trinitromethyl-substituted polynitro-pyrazoles: high-energy-density materials with positive oxygen balances†

Lujia Ding,[a] Ruirong Ge,[b] Pengcheng Wang,[a] Dongxue Li,[c] Qiuhan Lin,[a] Ming Lu *[a] and Yuangang Xu *[a]

An *N*-trinitromethyl strategy was employed for the synthesis of polynitro-pyrazole based high-energy-density compounds with great potential as energetic materials. The new compounds were characterized by ^{1}H and ^{13}C NMR, IR spectroscopy, elemental analysis, differential scanning calorimetry, and single-crystal X-ray diffraction. Compound **10** exhibits high energetic properties, has a positive oxygen balance (OB) of +2.1%, and an excellent specific impulse (272.4 s), making it a potential high-energy dense oxidizer to replace AP in solid rocket propellants. The nitration of **7** with HNO_3/H_2SO_4 yielded the green primary explosive **12**, which showed higher density, higher performance, better oxygen balance and lower sensitivities to those of currently used diazodinitrophenol. Compound **13** is a nitrogen and oxygen rich secondary explosive with a high OB (+5.0%), comparable energy (D = 9030 m s^{-1}; P = 35.6 GPa; η = 1.03) to HMX, and much lower mechanical sensitivity (IS = 12 J, FS = 240 N).

Received 29th September 2022
Accepted 14th November 2022

DOI: 10.1039/d2ra06149j

rsc.li/rsc-advances

Introduction

Energetic materials represent an important class of compounds that can rapidly release a large amount of energy when subjected to appropriate external stimuli to accomplish propulsion, damage and other purposes, and are widely used in civil and military applications.[1] Creating new nitrogen-rich, energetic compounds has been a long-standing goal of chemists and has attracted considerable interest due to the technical challenges involved in synthesis and isolation.[2] New high-energy-density materials (HEDMs) must meet increasing energy requirements, also considering oxygen balance, thermal stability and sensitivity.

In recent years, five-membered nitrogen-rich heterocyclic compounds (azoles) have emerged as the most promising skeleton for the design and synthesis of advanced HEDMs.[3] The azoles have a large number of N–N and C–N bonds and aromatic heterocycles, and their energy is released from the high positive heat of formation rather than by the oxidation of the carbon backbone as in traditional explosives (eg: TNT, TATB).[4] Therefore, azoles tend to have high energy density and good thermal stability. Among them, pyrazole is easy to carry out electrophilic substitution reactions such as nitration and halogenation due to the compactness, stability and modifiability of its own structure, and the density and nitrogen content of nitro-substituted pyrazole increase with the increase of the nitro group on the ring.[5] It can improve the detonation performance of the target compound. In recent years, many valuable nitropyrazole energetic compounds have been synthesized successively, such as 4-amino-3,5-dinitropyrazole (LLM-116), 3,6-dinitro-1,5-dihydropyrazolo[4,3-*c*]pyrazole (DNPP), and 3,4,5-trinitropyrazole (TNP).[6]

However, they have not yet found use as energetic materials due to the presence of strongly acidic N–H protons. Salt formation,[7] *N*-hydroxylation,[8] *N*-dinitromethylation,[9] *N*-trinitromethylation,[10] *N*-nitromethylation,[11] *N*,*N*′-alkyl bridge,[12] *N*-methylation,[13] *N*-amination[14] are among the various approaches that have been used to address this problem (Fig. 1). However, except for hydroxylation and di/tri-nitromethylation, the oxygen balances of nitropyrazoles cannot be improved, and the energy performances of the modified compounds are often reduced. Unfortunately, *N*-hydroxy derivatives were found to be generally very sensitive to impact, for example 3,4,5-trinitropyrazole-1-ol[15] was tested to be IS = 1 J. Therefore, in this work, we report the *N*-trinitromethylation of four nitropyrazoles, and the obtained six di/trinitromethyl-substituted energetic compounds. Most of these compounds were found to have detonation performances superior to that of RDX, positive oxygen balances and specific impulses higher than that of HMX.

[a]*School of Chemistry and Chemical Engineering, Nanjing University of Science and Technology, Xiaolingwei 200, Nanjing 210094, Jiangsu, China. E-mail: luming@njust.edu.cn; yuangangxu@163.com*

[b]*Anhui Hongxing Electrical Polytron Technologies Inc, Hefei 231135, Anhui, China*

[c]*China National Quality Inspection and Testing Center for Industrial Explosive Materials, Xiaolingwei 200, Nanjing 210094, Jiangsu, China*

† Electronic supplementary information (ESI) available. CCDC 2205049 (**2**), 2152126 (**6**), 2152131 (**7**), 2152133 (**10**), 1881963 (**11**), 2152132 (**12**), 2205042 (**13**), 2205048 (**14**), and 2205331 (**15**·2H_2O). For ESI and crystallographic data in CIF or other electronic format see DOI: https://doi.org/10.1039/d2ra06149j

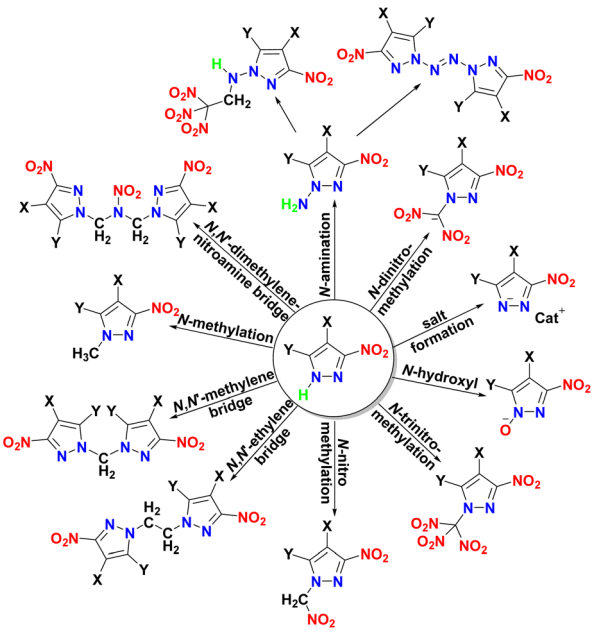

Fig. 1 Various approaches to remove the acidic N–H proton in nitropyrazole (X, Y: $-NO_2$, $-NH_2$, $-N_3$, –H, *etc.*).

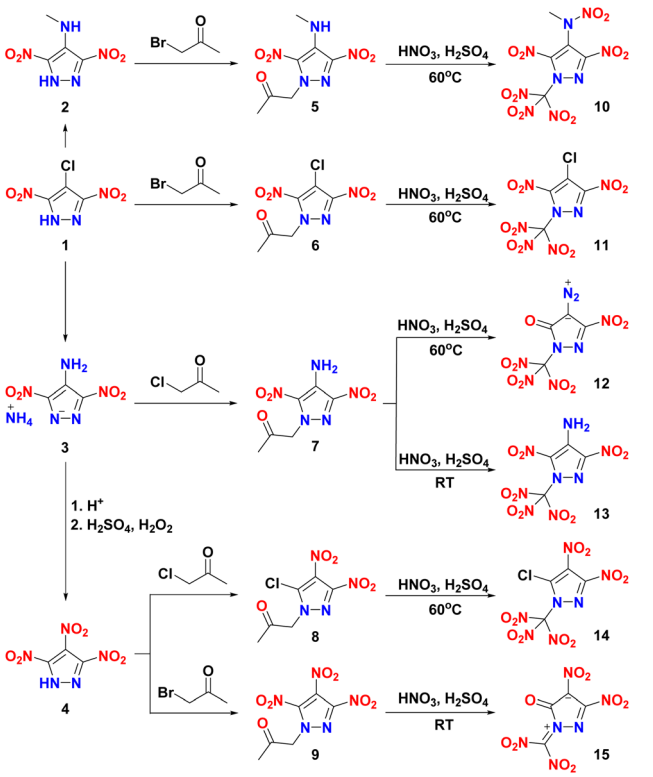

Scheme 1 Synthetic routes for compounds **10–15**.

Results and discussion

Synthesis

The synthetic routes are shown in Scheme 1. Compounds **1–4** were synthesized according to the literature.[5b,6c,12b] By the reaction of **1**, **2**, and **4** with bromoacetone under alkaline conditions, *N*-alkyl-functionalized nitropyrazoles **6**, **5**, and **9** were easily obtained in the yields of 86.5, 81.3, and 75.2%, respectively. While compounds 7 and **8** were obtained by reaction of **3** and **4** with KBr and chloroacetone in DMF at 70 °C. Compounds **5–8** were nitrated with a mixture of 98% H_2SO_4 and 98% HNO_3 for 2–5 h at 60 °C to give the corresponding trinitromethyl compounds **10–12** and **14**. Interestingly, when 7 was nitrated by the same mixed acid system at room temperature for 6 h, **13** was obtained in 44.9% yield. While **9** was treated similarly, *N*-dinitromethyl substituted **15** was obtained.

Single crystal X-ray diffraction

Crystals of **2**, **6**, **7**, and **10–15** suitable for single-crystal X-ray diffraction were obtained *via* the slow evaporation of their methanol or diethyl ether solution at room temperature, and their structures are shown in Fig. 2, and Fig. S1–S6.† Their crystallographic data, bond lengths, bond angles, and hydrogen bonds are given in the ESI.†

Compound **2** crystallizes in a monoclinic crystal system (space group *Pc*). Compound **6** and 7 all crystallizes in the monoclinic $P2_1c$ space group. Their C–C, C–N, and N–N bond lengths are normal in pyrazoles. Many hydrogen bonds can be clearly observed from their packing diagrams (Fig. S2, S4 and S6†).

Compound **10** crystallizes in the orthorhombic space group *Pbca* with a density of 1.894 g cm^{-3} at 150 K and eight molecules per unit cell. Its density is much higher than that of *N*-(3,5-

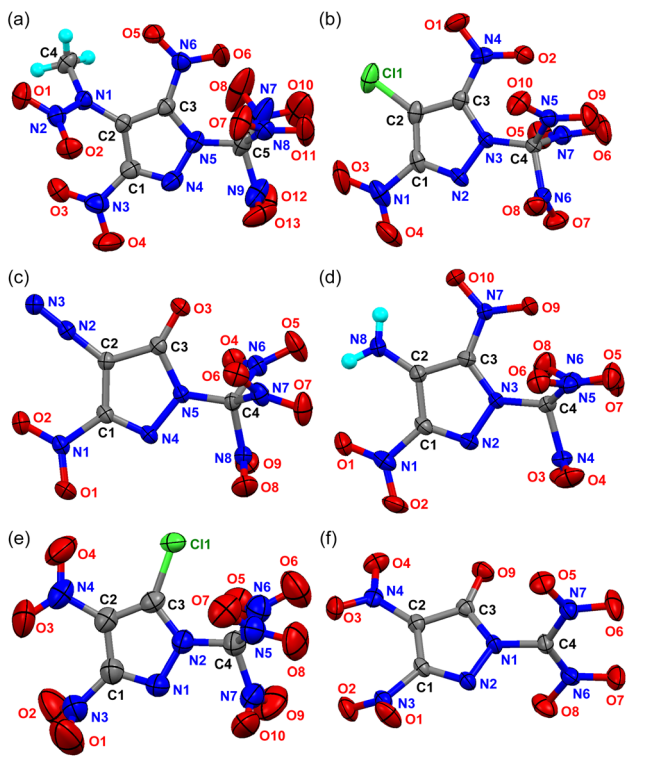

Fig. 2 Crystal structures of **10–15** (a–f). Thermal ellipsoids are drawn at the 50% probability level.

dinitro-1*H*-pyrazol-4-yl)-*N*-methylnitramide[5b] (1.74 g cm^{-3}). Only the nitro group attached to C3 is substantially coplanar with the pyrazole ring, which could be seen from the torsional angle of O6–N6–C3–N5 (2.59°) and O5–N6–C3–C2 (3.43°). The adjacent trinitromethyl group is staggered so that its two nearer nitro groups straddle the ring plane fairly symmetrically (see Fig. 2a). The nitrogen atom N9 of the other nitro group is almost in line with C1 and N4 on the pyrazole ring (N9–N4–C1: 172.39°), and the distance from N4 is 2.561 Å. Even in this optimal conformation, several nonbonding distances are significantly less than their corresponding van der Waals (*e.g.*, O6···N7 = 2.702 Å, O6···N8 = 2.757 Å, van der Waals O···N = 2.90 Å), which is a good indicator of repulsive strain. A comparison of bond angles provides further evidence of strain as bond angles near the close contact region are several degrees larger than the corresponding types of bond angles further away; *e.g.*, the closer trinitromethyl N–C–N angle is 112.32° (N7–C5–N8), while the farther ones are 105.85° (N7–C5–N9) and 104.65° (N8–C5–N9). Combining with the literature,[16] it is shown that the similar arrangement is formed when the trinitromethyl group is in the ortho position of the nitro group.

Compounds **11–13** all crystallize in the monoclinic space group $P2_1/n$. Their calculated densities are 1.960 g cm^{-3} (173 K), 1.927 g cm^{-3} (170 K), and 1.895 g cm^{-3} (193 K), higher than that of **10** (1.894 g cm^{-3} at 150 K). All substituents except trinitromethyl group in **11–13** are nearly coplanar with the pyrazole ring. The structural features of the trinitromethyl group in the three compounds are similar to those of **10**. Compared with 4-diazo-5-nitro-pyrazol-3-one,[17] the C=O bond in *N*-trinitromethyl-substituted compound **12** is shorter, but both the C–NO_2 and C–N_2^+ bonds are longer.

Compound **14** crystallizes in the monoclinic space group $P2_1/c$ with four molecules per unit cell and a calculated density of 1.859 g cm^{-3} at 296 K. Compound **15** crystallizes with two water molecules in the triclinic $P\bar{1}$ space group with two molecules per unit cell. The C1 and C2 positions of the pyrazole ring in compounds **14** and **15** are adjacent nitro groups, and the C3 position is an electronegative single atom (chlorine and oxygen). Due to steric hindrance, the nitro group at C2 twists slightly out of the plane of the pyrazole ring, while the nitro group at C1 has a larger twist angle.

A series of short intermolecular O···O and O···N contacts could be observed in the crystals, indicating the presence of weak interactions between the single molecules in the solid state. However, only a few hydrogen bonding interactions were found in **10**, **13** and **15**·$2H_2O$ (Fig. 3).

To gain more insight into the intermolecular interactions, two-dimensional (2D) fingerprints of crystals and the associated Hirshfeld surfaces (Fig. 4) were analyzed using Crystalexplorer 17.5 (ref. 18). The red and blue areas on the Hirshfeld surfaces represent high and low close contact populations, respectively. Fig. 4 shows red dots scattered in many orientations, mainly near the oxygen atoms of the trinitromethyl, nitro, and carbonyl groups, thus indicating strong intermolecular O···O, N···O, O···N, and O···C interactions. In addition to these interactions, compounds **11** and **14** have apparent Cl···O interactions between the chlorine and the oxygen atoms of the nitro groups

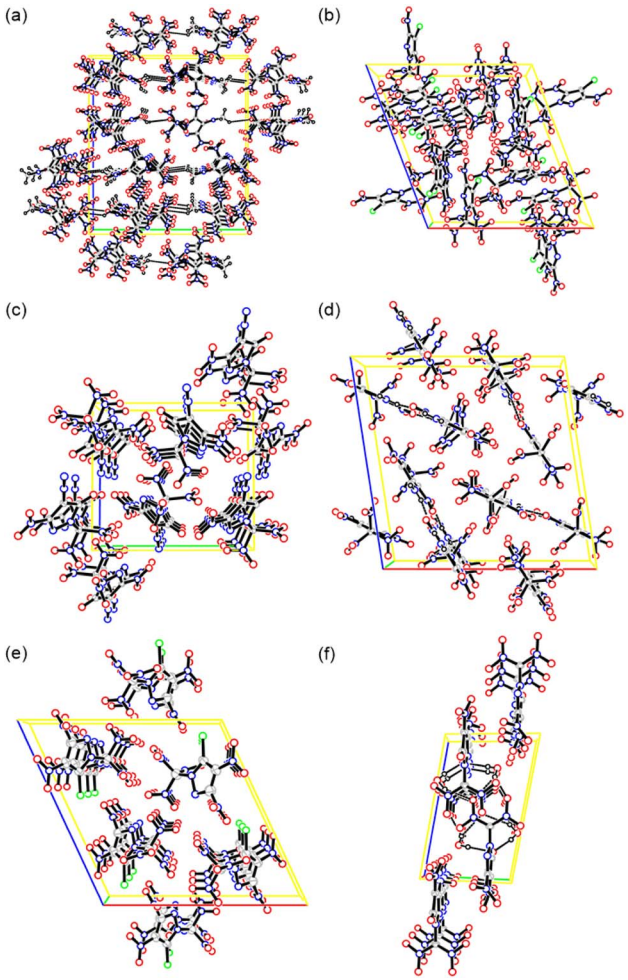

Fig. 3 Packing diagrams of **10–15** (a–f). Unit cell indicated and dashed lines represent hydrogen bonding.

in the adjacent molecule. Compounds **10**, **13** and **15** also have H···O interactions, that is, hydrogen bonds. Furthermore, in the 2D fingerprint plots of crystal **13** (Fig. 4k), a pair of spikes on bottom left (H···O & O···H interactions) indicate intermolecular hydrogen bonds. While, there is only one spike in **15**, because its molecule contains no hydrogen and only acts as hydrogen bond acceptors. According to the *di* + *de* values of the spikes, it can be seen that the O···H hydrogen bonds in **15** are stronger than the N···H hydrogen bonds in **13**. In fact, there are also weak O···H interactions in **10**, and their proportion (28.2%) is even higher than those (22.8%) in **13**. Except for compound **15**, the proportions of O···O interactions are more than 50%, indicating that compounds **10–14** are high dense. Since the oxygen atoms are in the trinitromethyl and nitro groups, higher proportion of close O···O contacts indicates that more nitro groups exposed on the molecular surface, may leading to an increased possibility of unexpected explosion.

Physicochemical and energetic properties

To identify the decomposition temperatures of high energy density compounds **10–15**, differential scanning calorimetry

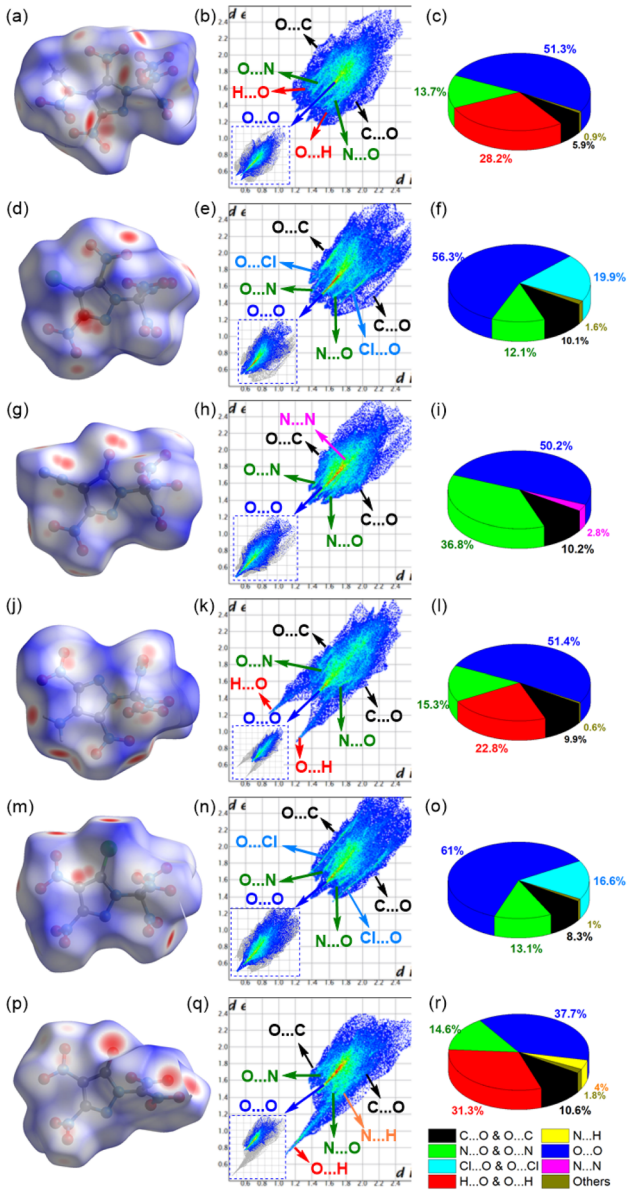

Fig. 4 (a–c) Hirshfeld surface, 2D fingerprint plot, and pie graph of the individual atomic contact percentage for **10**. (d–f) Hirshfeld surface, 2D fingerprint plot, and pie graph of the individual atomic contact percentage for **11**. (g–i) Hirshfeld surface, 2D fingerprint plot, and pie graph of the individual atomic contact percentage for **12**. (j–l) Hirshfeld surface, 2D fingerprint plot, and pie graph of the individual atomic contact percentage for **13**. (m–o) Hirshfeld surface, 2D fingerprint plot, and pie graph of the individual atomic contact percentage for **14**. (p–r) Hirshfeld surface, 2D fingerprint plot, and pie graph of the individual atomic contact percentage for **15**.

(DSC) with a heating rate of 5 °C min^{-1} was used. The results are shown in Fig. 5 and Table 1.

Among the six title compounds, only compounds **11** and **14** containing chlorine substituents have obvious endothermic peaks before decomposition, and the corresponding melting points were 72 °C (**11**) and 69 °C (**14**), respectively. All other compounds are directly decomposed without going through the melting process (Fig. 5). The decomposition temperatures of

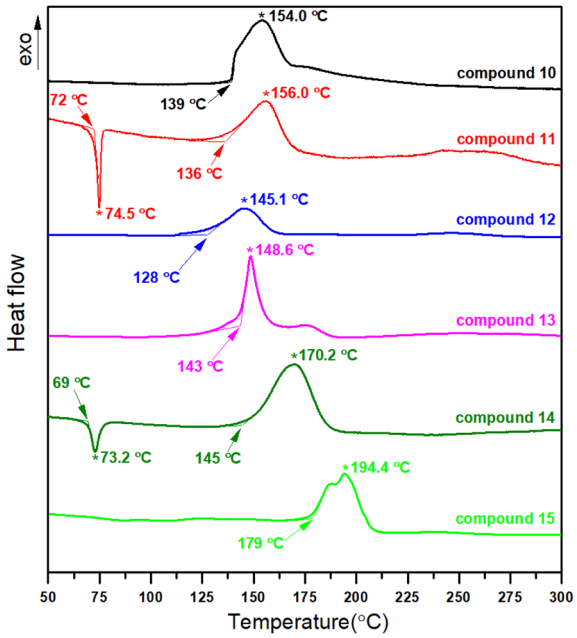

Fig. 5 DSC curves of compounds **10–15** measured with a heating rate of 5 °C min^{-1}.

10–14 range from 128 to 145 °C, which are consistent with the decomposition temperatures of most trinitromethyl functionalized compounds.[19] Compound **14**, as an isomer of **11**, has a decomposition temperature nearly 10 °C higher than that of **11**. *N*-dinitromethyl substituted nitropyrazole **15** are more thermally stable than all *N*-trinitromethyl substituted nitropyrazoles.

The mechanical sensitivities of compounds **10–15** toward impact (IS) and friction (FS) were determined by using a BAM drop hammer apparatus and BAM friction tester, respectively. The results are summarized in Table 1. Compound **12** (IS = 3 J, FS = 50 N) is the most sensitive among them, due to the structure of its diazonium inner salt. *N*-trinitromethyl makes its impact sensitivity higher than that of the unsubstituted 4-diazo-5-nitro-pyrazol-3-one (IS = 4.5 J),[17] but the friction sensitivity is slightly reduced. Six nitro groups are in one molecule of **10**, resulting in its impact and friction sensitivities of 5 J and 100 N. Other compounds have sensitivities ranging from 10–20 J and 180–240 N, which are more insensitive than RDX (7.5 J, 120 N) and HMX (7 J, 112 N).[20] It is worth mentioning that **13** has a "NO_2–NH_2–NO_2" structure similar to TATB and LLM-105, which may be an important reason for its lower sensitivity than 1-trinitromethyl-3,4,5-trinitropyrazole (7 J, 120 N).[10a]

The electrostatic potential (ESP) on the molecular surface here is used to analyze the relationship between molecular structure and impact sensitivity. The ESP-mapped vdW surfaces of **10–15** are shown in Fig. 6, with electron-rich areas marked blue and electron-deficient marked red. Surface local maxima and minima of ESP are represented as orange and cyan spheres, respectively. We can see that the positive electrostatic potential is mainly distributed near the pyrazole ring and the methyl, chlorine, amino and diazo groups. The negative electrostatic

Table 1 Physicochemical properties of **10**, **11**, **12**, **13**, **14** and **15**

Compound	Formula	T_d[a] [°C]	ρ[b] [g cm^{-3}]	ΔH_f[c] [kJ mol^{-1}]	D[d] [m s^{-1}]	P[e] [GPa]	IS[f] [J]	FS[g] [N]	OB(CO_2)[h] [%]	N[i] [%]	N + O[j] [%]	I_{sp}[k] [%]	η[l]
10	$C_5H_3N_9O_{12}$	139	1.853	516.67	9082	36.3	5	100	+2.1	33.08	83.45	272.4	1.04
11	$C_4ClN_7O_{10}$	136	1.924	457.47	8438	31.5	10	220	+11.7	28.71	75.55	251.4	0.98
12	$C_4N_8O_9$	128	1.891	479.75	9023	35.2	3	50	+5.3	36.85	84.20	263.7	1.04
13	$C_4H_2N_8O_{10}$	143	1.866	389.92	9030	35.6	12	240	+5.0	34.79	84.46	266.5	1.03
14	$C_4ClN_7O_{10}$	145	1.859	456.38	8184	29.0	15	200	+11.7	28.71	75.55	251.4	0.95
15	$C_4N_6O_9$	179	1.861	386.55	8821	33.7	20	180	+5.8	30.44	82.60	264.6	1.04
RDX[20]	$C_3H_6N_6O_6$	210	1.806	86.3	8801	33.6	7.5	120	−21.61	37.84	81.06	258	0.96
HMX[20]	$C_4H_8N_8O_8$	279	1.904	116.1	9193	37.8	7	112	−21.61	37.84	81.06	258	1.00

[a] Decomposition temperature (onset temperature from DSC at a heating rate of 5 °C min^{-1}). [b] Density, measured at 25 °C by a gas pycnometer. [c] Heat of formation. [d] Detonation velocity calculated by EXPLO5 V6.05.04. [e] Detonation pressure calculated by EXPLO5 V6.05.04. [f] Impact sensitivity. [g] Friction sensitivity. [h] Oxygen balance for $C_aH_bO_cN_d$, 1600(c-2a-b/2)/M_w; M_w = molecular weight. [i] Nitrogen content. [j] Nitrogen and oxygen content. [k] Specific impulse calculated by EXPLO5 V6.05.04. [l] Calculated metal acceleration ability by Muravyev–Wozniak–Piercey method.

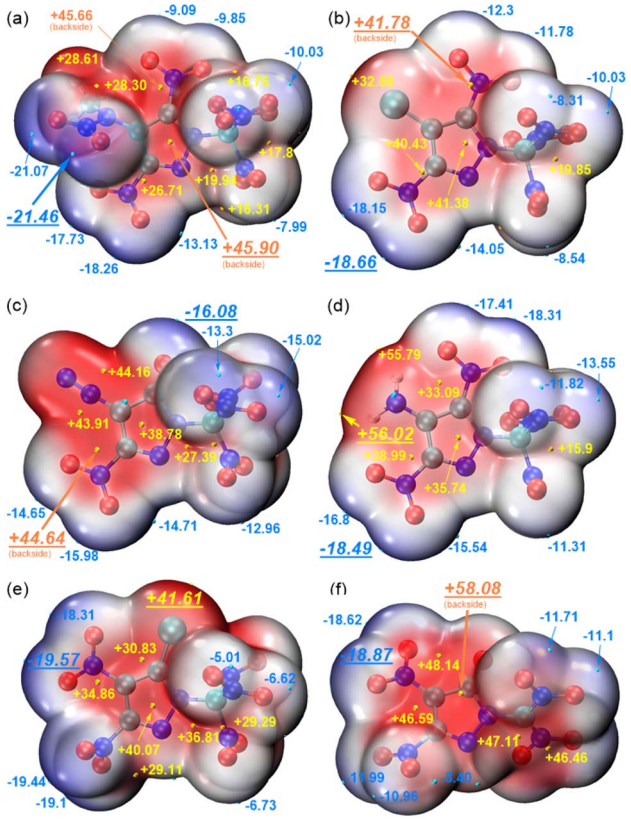

Fig. 6 The ESP-mapped vdW surfaces of **10–15** (a–f). ESP colour (blue-white-red) range from −0.04 to +0.04 Hartrees (a.u.).

potential is mainly distributed around the oxygen atoms of the nitro or carbonyl groups. According to the results of the Multiwfn[21] analysis, the average values of the positive electrostatic potential of the six compounds are greater than those of the negative electrostatic potential. The charge distribution of the molecular surface of impact-sensitive compounds corresponds to electron-poor areas above C–NO_2 bonds. Molecules that are more sensitive to impact have a larger electron deficiency (larger maxima of ESP) in this region than molecules that are less sensitive.[22] Compounds **12** and **10** show extremely intense electropositive areas, and the contrast is considerably stronger than others, which corresponds to the higher impact sensitivities and fits with the results of studies by Murray and Politzer.[23] It is worth mentioning that, the area of the positive potential region (128.7 Å^2) in **13** is slightly smaller than the negative potential region (129.4 Å^2), which is contrary to the general phenomenon in high energy density compounds. This may be an important reason for its relative insensitivity. For the dinitromethyl substituted **15**, the electron density appears to be more evenly distributed over the molecular surface than in the case for the trinitromethyl substituted **10–14**. This would account for a lower impact sensitivity of **15** (20 J) compared to **11–14** (3–15 J).

Their densities were determined at room temperature by a gas pycnometer to be 1.853 (**10**) to 1.924 g cm^{-3} (**11**), which are higher than that of RDX (1.80 g cm^{-3}). Heats of formation were calculated using the Gaussian 09 (Revision A.02) suite of programs[24] with isodesmic reactions (ESI†). Compounds **10–15** have relatively high positive heats of formation (ΔH_f) falling between 386.55 (**15**) and 516.67 (**10**) kJ mol^{-1}, which exceed both RDX (86.3 kJ mol^{-1}) and HMX (116.1 kJ mol^{-1}). Using the calculated ΔH_f values and the measured densities, the detonation parameters of **10–15** were calculated using the EXPLO5 V6.05.04 program.[25] Their detonation pressures (P) were predicted to be 29.0–36.3 GPa and the detonation velocities (D) is 8184–9082 m s^{-1}. Compounds **10**, **12**, **13**, and **15** exhibited higher detonation properties compared to RDX (P = 33.6 GPa, D = 8801 m s^{-1}).[20] In addition, the results calculated according to the Muravyev–Wozniak–Piercey method[26] show that compounds **10**, **12**, **13**, and **15** have slightly higher metal acceleration abilities (1.03–1.04) than HMX (1.00).

Energetic materials with a zero or positive oxygen balance (OB) convert all C into CO_2 and all H into H_2O. It is desirable that the energy can be completely released upon explosion while producing a minimal amount of toxic gas, so they can be considered "greener" than those with negative OBs.[27] The OB values of **10–15** are all positive (+2.1% to +11.7%), indicating that they are potential high-energy oxidizers for solid propellants. Therefore, specific impulse (I_{sp}), the most significant measure of the efficiency of a propellant (in seconds), was also calculated by using EXPLO5 V6.05.04.[25] Compounds **10**, **12**, **13**, and **15** have specific impulses of 263.7–272.4 s, which are much

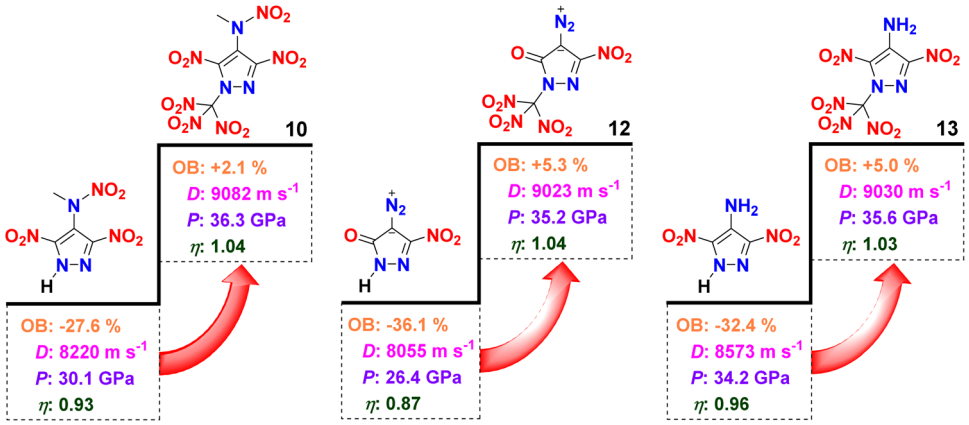

Fig. 7 Comparison of trinitromethyl substituted nitropyrazoles.

higher than those of AP (157 s),[19] ADN (202 s)[19] and HMX (258 s).[20]

Introduction of a *N*-trinitromethyl moiety is an effective way to enhance the OB of an energetic material. This is seen with the *N*-trinitromethyl substituted nitropyrazoles **10** (+2.1%), **12** (+5.3%), and **13** (+5.0%) having higher OB than their analogues *N*-(3,5-dinitro-1*H*-pyrazol-4-yl)-*N*-methylnitramide (−27.6%),[5b] 4-diazo-5-nitro-pyrazol-3-one (−36.1%),[17] and LLM-116 (−32.4%).[6b] In addition to the OB, their densities and heats of formation also increased to varying degrees (only the density of **13** decreased by 0.03 g cm^{-3}). In turn, their detonation velocities, detonation pressures, and metal acceleration abilities have all increased (Fig. 7). Taken together, these comparisons highlight the *N*-trinitromethyl strategy as an efficient functional modification to enhance OB and energy properties.

Conclusions

In conclusion, a series of *N*-trinitromethyl-substituted polynitro-pyrazoles were obtained by a simple and efficient synthesis, including *N*-acetomethylation followed by *N*-trinitromethylation. The novel compounds and their precursors were characterized by ^{1}H and ^{13}C NMR spectroscopy, elemental analysis, IR spectroscopy, and differential scanning calorimetry. The structures of **2**, **6**, **7**, and **10–15** were confirmed by single-crystal X-ray diffraction. Compound **10** exhibits excellent energetic performance (ρ = 1.853 g cm^{-3}; ΔH_f = 516.67 kJ mol^{-1}; D = 9082 m s^{-1}; P = 36.3 GPa), has a positive OB of +2.1%, and a promising specific impulse (272.4 s), making it an applicable high-energy dense oxidizer to replace AP in solid rocket propellants. The nitration of **7** with HNO_3/H_2SO_4 mixed acid generated *in situ* yielded the diazonium inner salt of polynitropyrazole **12**, the higher density, higher performance, better oxygen balance and lower sensitivity of which relative to diazodinitrophenol (DDNP) make it a competitive candidate as a green primary explosive. Compound **13** is a secondary explosive with a high OB (+5.0%), comparable energy (D = 9030 m s^{-1}; P = 35.6 GPa; η = 1.03) to HMX, and much lower sensitivity to external stimuli (IS = 12 J, FS = 240 N).

Experimental

Caution! All the nitro compounds are energetic materials. And they tend to explode unpredictably, under certain conditions. Caution should be exercised at all times during the handling of any of these compounds. Leather coat, ear protection, latex gloves, and face shield are strongly recommended for the experimental operation.

4-Chloro-3,5-dinitro-1*H*-pyrazole (**1**),[12b] *N*-methyl-3,5-dinitro-1*H*-pyrazol-4-amine (**2**),[5b] ammonium 4-amino-3,5-dinitropyrazole-1-ide (**3**),[12b] 3,4,5-trinitro-1*H*-pyrazole (**4**),[6c] 1-(4-amino-3,5-dinitro-1*H*-pyrazol-1-yl)propan-2-one (**7**),[9] and 1-(3,4,5-trinitro-1*H*-pyrazol-1-yl)propan-2-one (**9**)[28] were synthesized according to the literature.

1-(4-(Methylamino)-3,5-dinitro-1*H*-pyrazol-1-yl)propan-2-one (5)

A solution of bromoacetone (2.88 g, 21 mmol, 1.765 mL) in acetone (3 mL) was added drop-wise to a solution of compound **2** (3.74 g, 20 mmol) and NaOH (0.8 g, 20 mmol) in water (10 mL). The resulting mixture was stirred at room temperature for 18 h and a precipitate was isolated, which was washed with ice-water (20 mL), dried in air, giving **5** as a brown solid (3.95 g, 81.3%). T_m: 143 °C. ^{1}H NMR: δ 7.41, 7.40, 5.61, 2.98, 2.97, 2.26 ppm; ^{13}C NMR: δ 200.36, 141.71, 132.58, 130.69, 33.17, 26.93 ppm. IR (ATR): $\tilde{\nu}$ 3352, 2940, 2360, 1729, 1608, 1518, 1486, 1435, 1415, 1382, 1366, 1331, 1306, 1208, 1178, 1119, 1035, 898, 830, 815, 790, 745, 658, 611, 581 cm^{-1}. Elemental analysis for $C_7H_9N_5O_5$ (243.179): calcd C 34.57, H 3.73, N 28.80%. Found: C 34.49, H 3.66, N 28.72%.

1-(4-Chloro-3,5-dinitro-1*H*-pyrazol-1-yl)propan-2-one (6)

a solution of bromoacetone (2.88 g, 21 mmol, 1.765 mL) in acetone (3 mL) was added drop-wise to a solution of compound **1** (3.85 g, 20 mmol) and NaOH (0.8 g, 20 mmol) in water (10 mL). The resulting mixture was stirred at room temperature for 18 h and a precipitate was isolated, which was washed with ice-water (20 mL), dried in air, giving **6** as a white solid (4.30 g, 86.5%). T_m: 117 °C. ^{1}H NMR: δ 5.82, 2.32 ppm; ^{13}C NMR: δ 199.63,

148.66, 142.53, 106.13, 64.15, 26.96 ppm. IR (ATR): $\tilde{\nu}$ 3585, 3015, 2938, 2359, 1737, 1557, 1538, 1501, 1448, 1408, 1361, 1317, 1205, 1174, 1144, 1071, 1045, 993, 895, 826, 813, 789, 744, 685, 647, 631, 549 cm^{-1}. Elemental analysis for $C_6H_5ClN_4O_5$ (248.579): calcd C 28.99, H 2.03, N 22.54%. Found: C 28.92, H 2.11, N 22.48%.

1-(5-Chloro-3,4-dinitro-1*H*-pyrazol-1-yl)propan-2-one (8)

Compound **4** (0.609 g, 3 mmol) was dissolved in DMF (3 mL), followed by the addition of sodium bicarbonate (0.252 g, 3 mmol) and potassium bromide (0.357 g, 3 mmol) in stirring. The reaction system was heated to 70 °C, then chloroacetone (0.333 g, 3.6 mmol, 0.287 mL) was added drop-wise, and the reaction was maintained at 70 °C for 2 h. After cooling to room temperature, the reaction was quenched in cold water and a precipitate was isolated, which was washed with ice-water (20 mL), dried in air, giving **8** as a white solid (0.223 g, 29.9%). T_m: 131 °C. ^{1}H NMR: δ 5.61, 2.30 ppm; ^{13}C NMR: δ 199.12, 147.12, 131.34, 123.29, 60.12, 27.00 ppm. IR (ATR): $\tilde{\nu}$ 2999, 2954, 2184, 2173, 1993, 1965, 1731, 1538, 1506, 1428, 1400, 1361, 1336, 1310, 1200, 1174, 1071, 1061, 986, 900, 849, 833, 814, 795, 754, 698, 662, 648, 621, 587, 544 cm^{-1}. Elemental analysis for $C_6H_5ClN_4O_5$ (248.579): calcd C 28.99, H 2.03, N 22.54%. Found: C 29.06, H 2.09, N 22.49%.

N-(3,5-Dinitro-1-(trinitromethyl)-1*H*-pyrazol-4-yl)-*N*-methylnitramide (10)

Compound **5** (0.365 g, 1.5 mmol) was added to an ice-cold 98% H_2SO_4 (2.4 mL) and the mixture was stirred at 0–5 °C for 30 min. Then 98% HNO_3 (2.6 mL) was added drop-wise into the mixture at 0 °C. After slowly warming to room temperature, the mixture was heated to 60 °C. The final reaction was stirred at 60 °C for 2 h. After pouring into ice-water with vigorous stirring, the final mixture was filtered, washed with ice-water and dried in air, giving **10** as a white solid (0.40 g, 70.0%). T_d: 139 °C. ^{1}H NMR: δ 3.81 ppm; ^{13}C NMR: δ 206.56, 152.40, 142.14, 119.66, 41.22 ppm. IR (ATR): $\tilde{\nu}$ 3566, 2934, 2360, 1646, 1633, 1610, 1559, 1478, 1454, 1434, 1397, 1365, 1329, 1289, 1261, 1242, 1150, 1087, 1062, 991, 945, 862, 837, 822, 794, 766, 752, 667, 592, 562 cm^{-1}. Elemental analysis for $C_5H_3N_9O_{12}$ (381.130): calcd C 15.76, H 0.79, N 33.08%. Found: C 15.82, H 0.81, N 33.11%.

4-Chloro-3,5-dinitro-1-(trinitromethyl)-1*H*-pyrazole (11)

Compound **6** (1.39 g, 5.6 mmol) was added to an ice-cold 98% H_2SO_4 (6.0 mL) and the mixture was stirred at 0–5 °C for 30 min. Then 98% HNO_3 (6.5 mL) was added drop-wise into the mixture at 0 °C. After slowly warming to room temperature, the mixture was heated to 60 °C. The final reaction was stirred at 60 °C for 5 h. After pouring into ice-water with vigorous stirring, the final mixture was filtered, washed with ice-water and dried in air, giving **11** as a white solid (1.25 g, 65.4%). T_m: 72 °C; T_d: 136 °C. ^{13}C NMR: δ 206.91, 154.58, 144.41, 115.41 ppm. IR (ATR): $\tilde{\nu}$ 3586, 2935, 2360, 1737, 1646, 1627, 1606, 1575, 1533, 1428, 1390, 1314, 1257, 1167, 1090, 988, 857, 830, 816, 792, 762, 745, 724, 629, 576 cm^{-1}. Elemental analysis for $C_4ClN_7O_{10}$ (341.533): calcd C 14.07, N 28.71%. Found: C 14.16, N 28.78%.

4-Diazo-5-nitro-2-(trinitromethyl)-2,4-dihydro-3*H*-pyrazol-3-one (12)

Compound **7** (0.343 g, 1.5 mmol) was added to an ice-cold 98% H_2SO_4 (2.4 mL) and the mixture was stirred at 0–5 °C for 30 min. Then 98% HNO_3 (2.6 mL) was added drop-wise into the mixture at 0 °C. After slowly warming to room temperature, the mixture was heated to 60 °C. The final reaction was stirred at 60 °C for 3 h. After pouring into ice-water with vigorous stirring, the final mixture was filtered, washed with ice-water and dried in air, giving **12** as a white solid (0.316 g, 69.3%). T_d: 128 °C. ^{13}C NMR: δ 158.75, 155.20, 150.62, 123.47 ppm. IR (ATR): $\tilde{\nu}$ 3501, 2934, 2359, 2197, 1751, 1634, 1596, 1542, 1482, 1446, 1389, 1357, 1319, 1262, 1193, 1156, 1061, 1023, 995, 860, 837, 822, 792, 763, 725, 696, 674, 638, 606, 567 cm^{-1}. Elemental analysis for $C_4N_8O_9$ (304.091): calcd C 15.80, N 36.85%. Found: C 15.73, N 36.82%.

3,5-Dinitro-1-(trinitromethyl)-1*H*-pyrazol-4-amine (13)

Compound **7** (0.343 g, 1.5 mmol) was added to an ice-cold 98% H_2SO_4 (2.4 mL) and the mixture was stirred at 0–5 °C for 30 min. Then 98% HNO_3 (2.6 mL) was added drop-wise into the mixture at 0 °C. After slowly warming to room temperature within 2 h, the final reaction was stirred at room temperature for 6 h. After pouring into ice-water with vigorous stirring, the insoluble impurities were filtered off, and the filtrate was left to stand for 12 h, and a large amount of precipitates were formed. Washed with ice-water and dried in air, giving **13** as a pale solid (0.217 g, 44.9%). T_d: 143 °C. ^{1}H NMR: δ 8.07 ppm; ^{13}C NMR: δ 206.41, 148.76, 133.18, 130.74 ppm. IR (ATR): $\tilde{\nu}$ 3675, 3484, 3361, 2987, 2901, 2199, 1756, 1659, 1633, 1618, 1599, 1578, 1539, 1469, 1388, 1310, 1265, 1224, 1066, 1052, 975, 863, 838, 820, 794, 758, 738, 691, 655, 639, 597 cm^{-1}. Elemental analysis for $C_4H_2N_8O_{10}$ (322.106): calcd C 14.92, H 0.63, N 34.79%. Found: C 14.99, H 0.66, N 34.85%.

5-Chloro-3,4-dinitro-1-(trinitromethyl)-1*H*-pyrazole (14)

Compound **8** (1.39 g, 5.6 mmol) was added to an ice-cold 98% H_2SO_4 (6.0 mL) and the mixture was stirred at 0–5 °C for 30 min. Then 98% HNO_3 (6.5 mL) was added drop-wise into the mixture at 0 °C. After slowly warming to room temperature, the mixture was heated to 60 °C. The final reaction was stirred at 60 °C for 3 h. After pouring into ice-water with vigorous stirring, the final mixture was filtered, washed with ice-water and dried in air, giving **14** as a white solid (1.07 g, 56.1%). T_m: 69 °C; T_d: 145 °C. ^{13}C NMR: δ 206.25, 151.88, 136.72, 124.90 ppm. IR (ATR): $\tilde{\nu}$ 2887, 1966, 1621, 1606, 1563, 1537, 1487, 1456, 1361, 1328, 1265, 1140, 1084, 981, 965, 863, 834, 812, 791, 764, 701, 662, 634, 623, 599, 571, 565, 551 cm^{-1}. Elemental analysis for $C_4ClN_7O_{10}$ (341.533): calcd C 14.07, N 28.71%. Found: C 14.12, N 28.76%.

1-(Dinitromethylene)-3,4-dinitro-5-oxo-4,5-dihydro-1*H*-pyrazol-1-ium-4-ide (15)

Compound **9** (0.389 g, 1.5 mmol) was added to an ice-cold 98% H_2SO_4 (2.4 mL) and the mixture was stirred at 0–5 °C for 30 min. Then 98% HNO_3 (2.6 mL) was added drop-wise into the mixture at 0 °C. After slowly warming to room temperature within 2 h,

the final reaction was stirred at room temperature for 6 h. After pouring into ice-water with vigorous stirring, the solution was left to stand for 12 h, a small amount of precipitates were formed. Washed with ice-water and dried in air, giving **15** as a white solid (0.154 g, 37.2%). T_d: 179 °C. ^{13}C NMR: δ 200.33, 140.25, 131.54, 130.15 ppm. IR (ATR): $\tilde{\nu}$ 1635, 1511, 1372, 1318, 1279, 1122, 1044, 824, 756, 559 cm^{-1}. Elemental analysis for $C_4N_6O_9$ (276.077): calcd C 17.40, N 30.44%. Found: C 17.33, N 30.51%.

Conflicts of interest

There are no conflicts to declare.

Acknowledgements

Financial support of this work is provided by the National Natural Science Foundation of China (No. 22105102, and No. 21975127), the Young Elite Scientist Sponsorship Program by CAST (no. YESS20210074), and the Fundamental Research Funds for the Central Universities (No. 30921011204).

Notes and references

1 (*a*) M. B. Talawar, R. Sivabalan, T. Mukundan, H. Muthurajan, A. K. Sikder, B. R. Gandhe and A. Subhananda Rao, *J. Hazard. Mater.*, 2009, **161**, 589–607; (*b*) D. G. Piercey, D. E. Chavez, B. L. Scott, G. H. Imler and D. A. Parrish, *Angew. Chem., Int. Ed.*, 2016, **55**, 15315–15318.

2 (*a*) T. M. Klapötke, C. Petermayer, D. G. Piercey and J. Stierstorfer, *J. Am. Chem. Soc.*, 2012, **134**, 20827–20836; (*b*) P. Yin, Q. Zhang and J. M. Shreeve, *Acc. Chem. Res.*, 2016, **49**, 4–16; (*c*) W. Zhang, J. Zhang, M. Deng, X. Qi, F. Nie and Q. Zhang, *Nat. Commun.*, 2017, **8**, 181; (*d*) P. Yin, J. Zhang, G. H. Imler, D. A. Parrish and J. M. Shreeve, *Angew. Chem., Int. Ed.*, 2017, **56**, 8834–8838.

3 (*a*) H. Gao and J. M. Shreeve, *Chem. Rev.*, 2011, **111**, 7377–7436; (*b*) A. A. Dippold and T. M. Klapötke, *J. Am. Chem. Soc.*, 2013, **135**, 9931–9938.

4 (*a*) Y. Qu and S. P. Babailov, *J. Mater. Chem. A*, 2018, **6**, 1915–1940; (*b*) Y. Zhang, Y. Li, J. Hu, Z. Ge, C. Sun and S. Pang, *Dalton Trans.*, 2019, **48**, 1524–1529.

5 (*a*) S. Zhang, Z. Gao, D. Lan, Q. Jia, N. Liu, J. Zhang and K. Kou, *Molecules*, 2020, **25**, 3475; (*b*) C. He, J. Zhang, D. A. Parrish and J. M. Shreeve, *J. Mater. Chem. A*, 2013, **1**, 2863–2868; (*c*) M. Deng, Y. Feng, W. Zhang, X. Qi and Q. Zhang, *Nat. Commun.*, 2019, **10**, 1339; (*d*) H. Huang, Y. Shi, H. Li, H. Li, A. Pang and J. Yang, *Org. Lett.*, 2020, **22**, 5866–5869.

6 (*a*) S. Ek and N. V. Latypov, *J. Heterocycl. Chem.*, 2014, **51**, 1621–1627; (*b*) M. Zhang, P. F. Pagoria, G. H. Imler and D. Parrish, *J. Heterocycl. Chem.*, 2019, **56**, 781–787; (*c*) G. Hervé, C. Roussel and H. Graindorge, *Angew. Chem., Int. Ed.*, 2010, **49**, 3177–3181; (*d*) Y. Li, Y. Shu, B. Wang, S. Zhang and L. Zhai, *RSC Adv.*, 2016, **6**, 84760–84768; (*e*) W. Zhang, H. Xia, R. Yu, J. Zhang, K. Wang and Q. Zhang, *Propellants, Explos., Pyrotech.*, 2020, **45**, 546–553; (*f*) P. Yin, J. Zhang, L. A. Mitchell, D. A. Parrish and J. M. Shreeve, *Angew. Chem., Int. Ed.*, 2016, **55**, 12895–12897.

7 (*a*) Y. Feng, J. Wang and Z. Li, *Cryst. Growth Des.*, 2021, **21**, 4725–4731; (*b*) Y. Zhang, Y. Huang, D. A. Parrish and J. M. Shreeve, *J. Mater. Chem.*, 2011, **21**, 6891–6897; (*c*) M. F. Bölter, A. Harter, T. M. Klapötke and J. Stierstorfer, *ChemPlusChem*, 2018, **83**, 804–811.

8 (*a*) P. Yin, L. A. Mitchell, D. A. Parrish and J. M. Shreeve, *Chem.–Asian J.*, 2017, **12**, 378–384; (*b*) P. Yin, L. A. Mitchell, D. A. Parrish and J. M. Shreeve, *Angew. Chem., Int. Ed.*, 2016, **55**, 14409–14411.

9 B. Guo, X. Zhang, X. Lin, H. Huang and J. Yang, *New J. Chem.*, 2021, **45**, 20426–20431.

10 (*a*) W. Zhang, Y. Yang, Y. Wang, T. Fei, Y. Wang, C. Sun and S. Pang, *Chem. Eng. J.*, 2023, **451**, 138609; (*b*) I. L. Dalinger, I. A. Vatsadze, T. K. Shkineva, A. V. Kormanov, M. I. Struchkova, K. Yu. Suponitsky, A. A. Bragin, K. A. Monogarov, V. P. Sinditskii and A. B. Sheremetev, *Chem.–Asian J.*, 2015, **10**, 1987–1996.

11 D. Kumar, G. H. Imler, D. A. Parrish and J. M. Shreeve, *J. Mater. Chem. A*, 2017, **5**, 10437–10441.

12 (*a*) J. Zhang, C. He, D. A. Parrish and J. M. Shreeve, *Chem.–Eur. J.*, 2013, **19**, 8929–8936; (*b*) D. Fischer, J. L. Gottfried, T. M. Klapötke, K. Karaghiosoff, J. Stierstorfer and T. G. Witkowski, *Angew. Chem., Int. Ed.*, 2016, **55**, 16132–16135; (*c*) P. Yin, J. Zhang, D. A. Parrish and J. M. Shreeve, *Chem.–Eur. J.*, 2014, **20**, 16529–16536.

13 (*a*) I. L. Dalinger, I. A. Vatsadze, T. K. Shkineva, G. P. Popova, S. A. Shevelev and Y. V. Nelyubina, *J. Heterocycl. Chem.*, 2013, **50**, 911–924; (*b*) P. Yin, C. He and J. M. Shreeve, *J. Mater. Chem. A*, 2016, **4**, 1514–1519.

14 (*a*) P. Yin, J. Zhang, C. He, D. A. Parrish and J. M. Shreeve, *J. Mater. Chem. A*, 2014, **2**, 3200–3208; (*b*) G. Li, H. Huang, J. Yang, C. Yan, W. Li and H. Duan, *Polyhedron*, 2021, **199**, 115098; (*c*) P. Yin, D. A. Parrish and J. M. Shreeve, *Chem.–Eur. J.*, 2014, **20**, 6707–6712.

15 Y. Zhang, D. A. Parrish and J. M. Shreeve, *J. Mater. Chem.*, 2012, **22**, 12659–12665.

16 Y. Xu, C. Shen, Q. Lin, P. Wang, C. Jiang and M. Lu, *J. Mater. Chem. A*, 2016, **4**, 17791–17800.

17 Y. Du, J. Zhang, P. Peng, H. Su, S. Li and S. Pang, *New J. Chem.*, 2017, **41**, 9244–9249.

18 M. A. Spackman and D. Jayatilaka, *CrystEngComm*, 2009, **11**, 19–32.

19 Q. Yu, F. Li, P. Yin, S. Pang, R. J. Staples and J. M. Shreeve, *J. Mater. Chem. A*, 2021, **9**, 24903–24908.

20 N. Fischer, D. Fischer, T. M. Klapötke, D. G. Piercey and J. Stierstorfer, *J. Mater. Chem.*, 2012, **22**, 20418–20422.

21 T. Lu and F. Chen, *J. Comput. Chem.*, 2012, **33**, 580–592.

22 A. Hammerl, T. M. Klapötke, H. Nöth and M. Warchhold, *Propellants, Explos., Pyrotech.*, 2003, **28**, 165–173.

23 (*a*) J. S. Murray, M. C. Concha and P. Politzer, *Mol. Phys.*, 2009, **107**, 89–97; (*b*) P. Politzer, J. S. Murray, J. M. Seminario, P. Lane, M. E. Grice and M. C. Concha, *THEOCHEM*, 2001, **573**, 1–10.

24 M. J. Frisch, G. W. Trucks, H. B. Schlegel, G. E. Scuseria, M. A. Robb, J. R. Cheeseman, G. Scalmani, V. Barone,

B. Mennucci, G. A. Petersson, H. Nakatsuji, M. Caricato, X. Li, H. P. Hratchian, A. F. Izmaylov, J. Bloino, G. Zheng, J. L. Sonnenberg, M. Hada, M. Ehara, K. Toyota, R. Fukuda, J. Hasegawa, M. Ishida, T. Nakajima, Y. Honda, O. Kitao, H. Nakai, T. Vreven, J. A. Montgomery Jr., J. E. Peralta, F. Ogliaro, M. Bearpark, J. J. Heyd, E. Brothers, K. N. Kudin, V. N. Staroverov, R. Kobayashi, J. Normand, K. Raghavachari, A. Rendell, J. C. Burant, S. S. Iyengar, J. Tomasi, M. Cossi, N. Rega, J. M. Millam, M. Klene, J. E. Knox, J. B. Cross, V. Bakken, C. Adamo, J. Jaramillo, R. Gomperts, R. E. Stratmann, O. Yazyev, A. J. Austin, R. Cammi, C. Pomelli, J. W. Ochterski, R. L. Martin, K. Morokuma, V. G. Zakrzewski, G. A. Voth, P. Salvador, J. J. Dannenberg, S. Dapprich, A. D. Daniels, O. Farkas, J. B. Foresman, J. V. Ortiz, J. Cioslowski and D. J. Fox, *Gaussian 09, Revision A.02*, Gaussian, Inc., Wallingford, CT, 2009.

25 M. Sućeska, *EXPLO5 V6.05.04*, Brodarski Institute, Zagreb, Croatia, 2020.

26 N. V. Muravyev, D. R. Wozniak and D. G. Piercey, *J. Mater. Chem. A*, 2022, **10**, 11054–11073.

27 C. He and J. M. Shreeve, *Angew. Chem., Int. Ed.*, 2016, **55**, 772–775.

28 S. Zhang, F. Wang, X. Li, K. Yu, X. Qiu, C. Zhu and Z. Zhou, *Chinese invention Pat.*, CN114149372A, 2021.